COMPARISON OF BOUNDARY ELEMENT AND FINITE ELEMENT METHODS FOR LINEAR STRESS ANALYSIS - TECHNICAL PROGRAM RESULTS

Arturo Wanderlingh

Specialist Applied Numerical Analysis, Applied Mechanics Group, Hamilton Standard, Division of United Technologies Corporation, Windsor Locks, CT 06096

INTRODUCTION

Over the years, engineering organizations have become increasingly dedicated to improving productivity through the use of high-speed computers, computer-aided design and manufacturing (CAD/CAM) techniques and computer-aided analysis methods such as the Finite Element Method. Despite the analytical method's substantial impact on productivity, three limiting factors persist: 1) the difficulty in identifying connectivity errors, particularly in 3D models, 2) the need to discretize the entire volume of a structure, and 3) the density of the mesh needed to obtain accurate surface stresses. A numerical technique which has a potential for eliminating these shortcomings is the Boundary Element Method. The purpose of this paper is to discuss the results of a technical program conducted at Hamilton Standard, comparing the Boundary Element and Finite Element Methods for two- and three-dimensional, linear structural analyses.

APPROACH

Three classes of linear, static, room-temperature stress applications were analyzed: 2D axisymmetric (body of revolution) stress, 2D plane stress, and 3D stress. The usefulness of the Boundary Element Method for these applications was determined in the categories of model generation time, analysis solution time, solution convergence and data reduction. The boundary element program BEASY, an in-house finite element program, and MSC/NASTRAN were used to perform this study.

MODEL DESCRIPTION

2D Axisymmetric Stress - Both the barrel and cover of a typical actuator were constructed; see Figure 1. The actuator barrel consists of 350 constant strain elements and the cover consists of 529 elements. The applied boundary conditions are also shown in this figure. The boundary element models of this structure are shown in Figure 2. Twenty-eight quadratic elements represent the barrel and 64 elements define the cover.

2D Plane Stress - An internal spur gear tooth was modeled for this case; see Figure 3. The gear tooth model consists of 1,060 constant strain elements. A point load was applied to the tooth pitch diameter and the tooth boundary was completely constrained. The boundary element model, shown in Figure 4, consists of 41 quadratic elements.

3D Stress - One-eigth of a thick walled cylinder was selected for the 3D analysis; see Figure 5. The finite element model shown consists of 240 linear strain elements and is subjected to an internal pressure of 100 psi. The boundary element model shown in Figure 6 consists of 12 quadratic discontinous elements.

PROGRAM RESULTS

Axisymmetric Analysis - A comparison of the boundary element and finite element surface stress for the actuator barrel is shown in Figure 7. The maximum boundary element stress is 9% lower than the finite element solution. The boundary element stresses shown represent mesh point average values. When the difference between element stress contributions at a mesh point is 20% or greater, the BEASY program warns the analyst that a mesh refinement is required. Several boundary stress values, including the peak stress, were identified as having a mesh point average of 20% or greater.

Surface stress results for the cover are shown in Figures 8 and 9. The boundary element model in the vicinity of point D, shown in Figure 8, would require a mesh refinement to obtain correlation with the finite element solution. To better determine the stresses between points A and B, shown in Figure 9, a mesh refinement was made for both the finite element and boundary element models. While the refined boundary element peak stress (14 KSI) is substantially lower than the refined finite element peak stress (19 KSI), the boundary element mesh point average stress solution indicates that the true peak stress may be significantly higher ($\approx$27 KSI).

Plane Stress Analysis - Surface stresses, along with tooth fillet, are shown in Figure 10. The boundary element peak stress is 5% higher than that of the finite element result. These results were also compared to a modified Heywood Method, described in Reference 1, which is based on photo-elastic tests. The peak boundary element stress is 15% higher than the strength of materials method.

A further comparison was made of the internal stresses obtained from both the Finite Element and Boundary Element Methods; see Figure 11. The two methods correlated very well.

2D Modeling and Solution Time - Modeling and computer solution times are summarized for the axisymmetric and the plane stress models in Figure 12. All the analyses were performed on an IBM 3084 computer. The computer times listed are for the original models analyzed. The average modeling time using the BEASY preprocessor was approximately three times faster than the finite element modeling time. However, the Boundary Element Method, on the average, used approximately twice as much computer time than the Finite Element Method.

2D Convergence - Several additional models of the internal spur gear tooth were constructed to determine surface stress sensitivity to mesh size; see Figure 13. The density of the finite element meshes was increased in the vicinity of the tooth fillet until the peak fillet stress did not change more than 5%. While the initial boundary element solution indicated convergence, two additional runs were made for the purpose of confirmation. Convergence results are shown in Figure 14. The computer times of the converged finite element models range from 3 to 15 times higher than the initial boundary solution. This represents a more reasonable computer time comparison between the two methods then the previous 2D cases because it is based on the same degree of stress accuracy.

3D Stress - Stresses on the inner diameter of the cylinder are summarized in Figure 15. A strength of materials calculation, obtained from Reference 2, is also tabulated. The finite element solution took 1.4 times longer to obtain the same accuracy in radial surface stress as the Boundary Element Method. However, the Finite Element Method took 130 cpu seconds less time to obtain a radial displacement, which is less than 5% of the theoretical value.

CONCLUSION

Use of the Boundary Element Method can favorably impact engineering productivity by significantly reducing the model generation and data reduction time. Since the Boundary Element Method does not require the discretization of the interior portion of a structure, fewer, if any, errors of geometry are made. Typically, determination of surface stresses is a primary objective in structural analysis. The Boundary Element Method produces surface stresses in a form which is more easily extracted and interpreted than the Finite Element Method. Also, the mesh point averaging technique, used in BEASY, indicates the accuracy of the solution, thereby, increasing the analyst's confidence in the results. The Boundary Element Method, unlike the Finite Element Method, calculates stresses and displacements directly, thus yielding the same order of accuracy for both. In principle, this means orders of magnitude less boundary elements are required than finite elements for determining stress. Use of the discontinuous boundary elements, as in the case of the 3D cylinder model, allows further reductions in mesh size and modeling time without reducing solution accuracy.

For the classes of structural applications analyzed, the boundary element computer solution time is comparable to the finite element time. Depending on the solution accuracy desired, the boundary element solution can take less time than the Finite Element Method.

One area which requires scrutiny is the analysis of highly complex three-dimensional structures which require a large number of elements. There may exist a point where the time saved in the generation of the model is offset by the computer solution time.

REFERENCES

1. Cornell, R. W. (1981) "Compliance and Stress Sensitivity of Spur Gear Teeth", Journal of Mechanical Design, Vol. 103: 447-459.

2. Roark, A. J., "Formulas for Stress and Strain", Fifth edition, page 504, case 1, 1975.

<u>FIGURE 1</u>

<u>ACTUATOR FINITE ELEMENT MODELS</u>

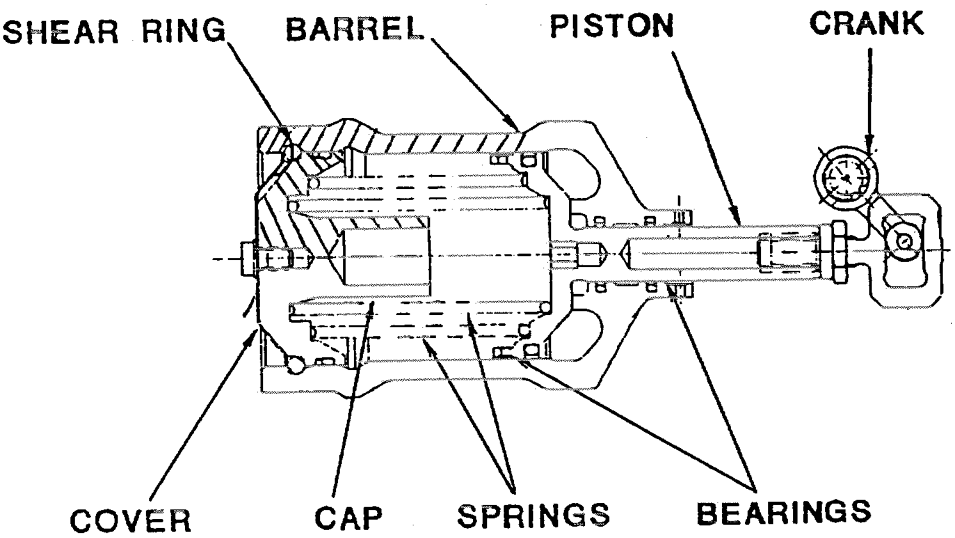

<u>Barrel</u>

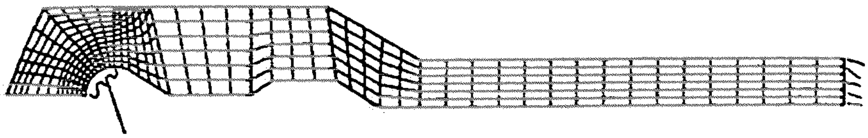

Linearly varying pressure from shear ring

<u>Cover</u>

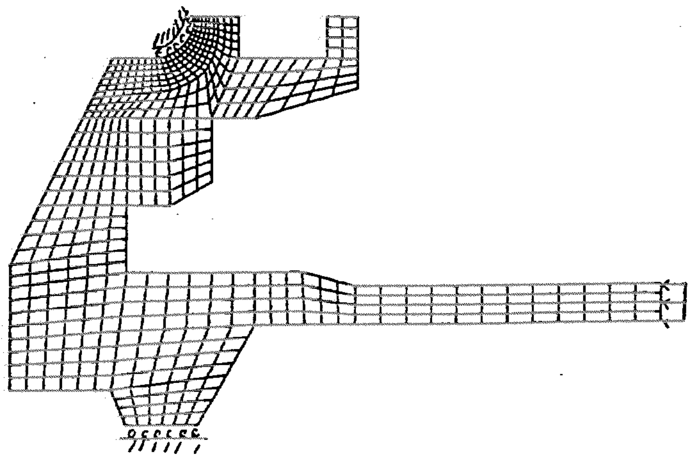

FIGURE 2

ACTUATOR BOUNDARY ELEMENT MODELS

28 Boundary Elements

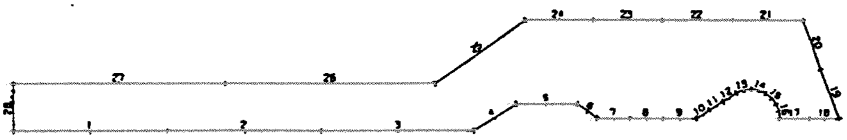

Barrel

64 Boundary Elements

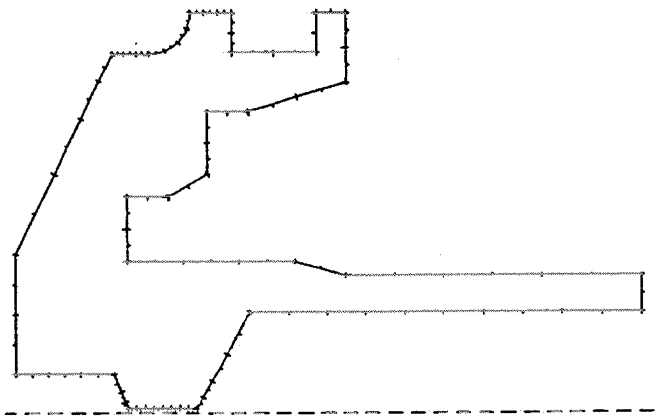

Cover

FIGURE 3

FINITE ELEMENT MODEL OF INTERNAL SPUR GEAR TOOTH

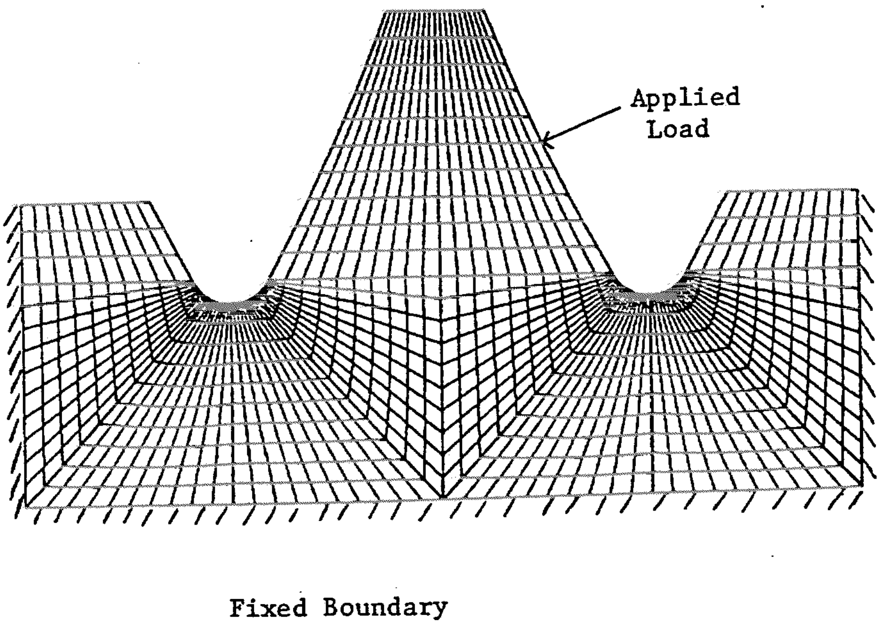

FIGURE 4

BOUNDARY ELEMENT MODEL OF INTERNAL SPUR GEAR TOOTH

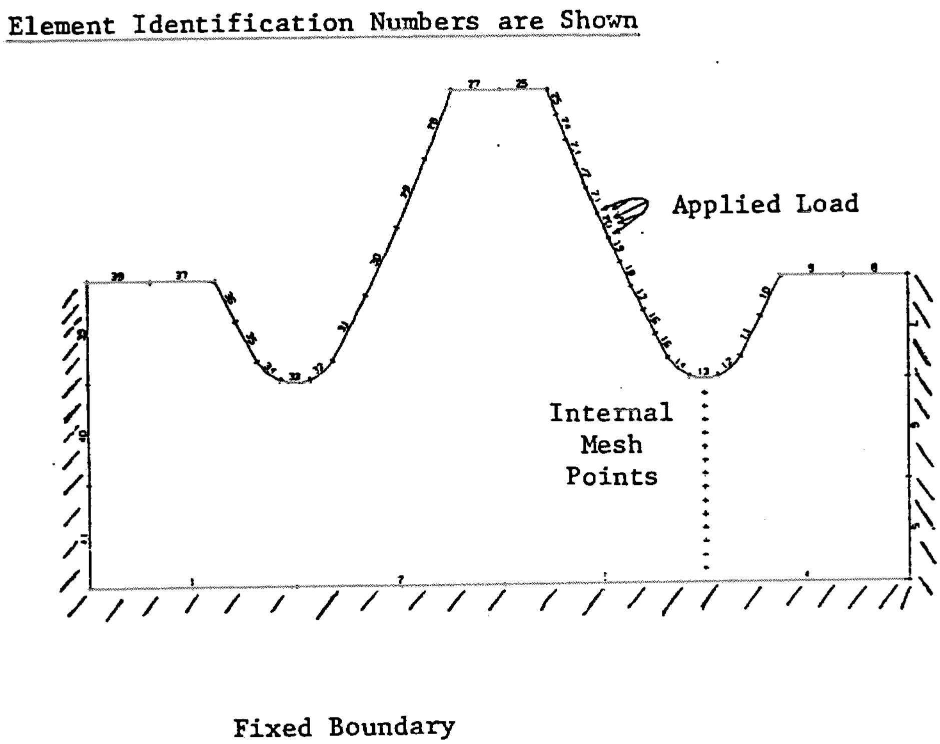

FIGURE 5

FINITE ELEMENT MODEL OF A THICK WALL CYLINDER

1/8th Segment of Cylinder

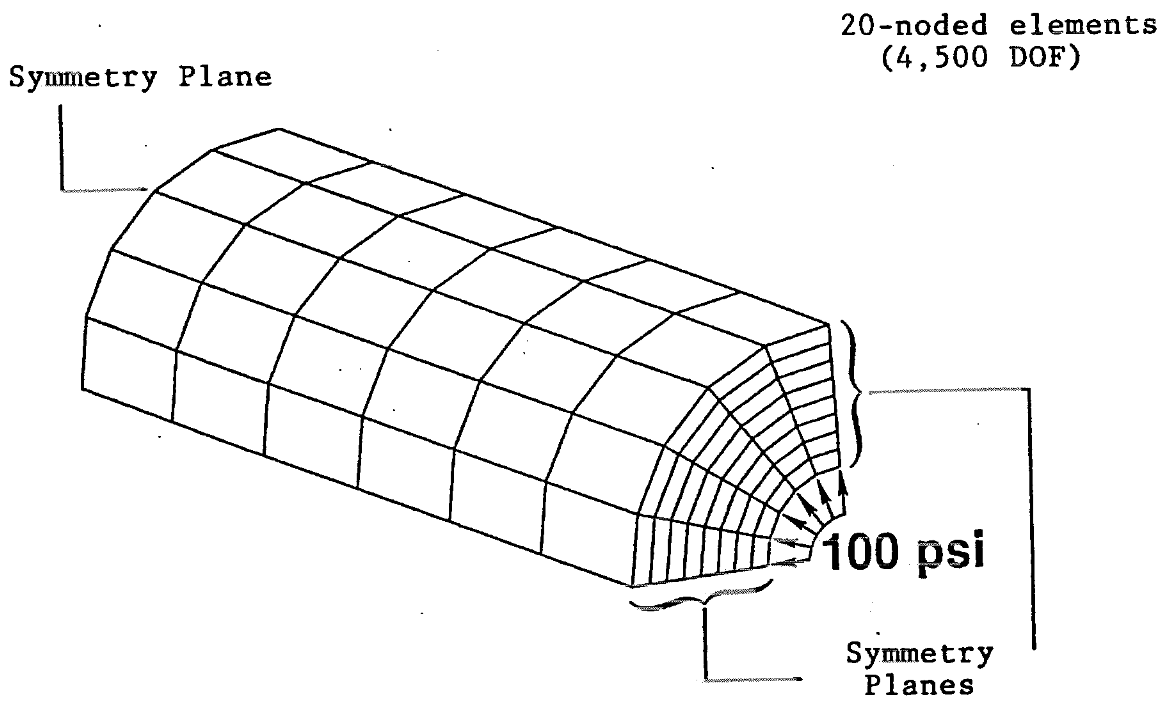

FIGURE 6

BOUNDARY ELEMENT CYLINDER MODEL

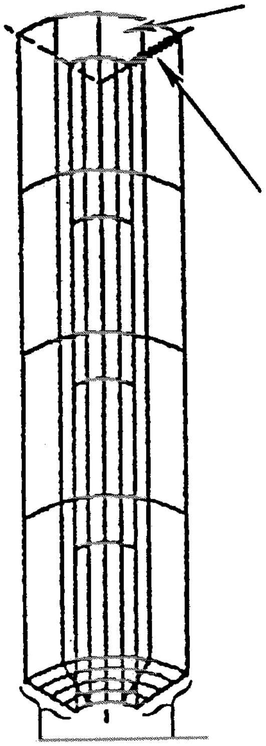

FIGURE 7

ACTUATOR BARREL SURFACE STRESS

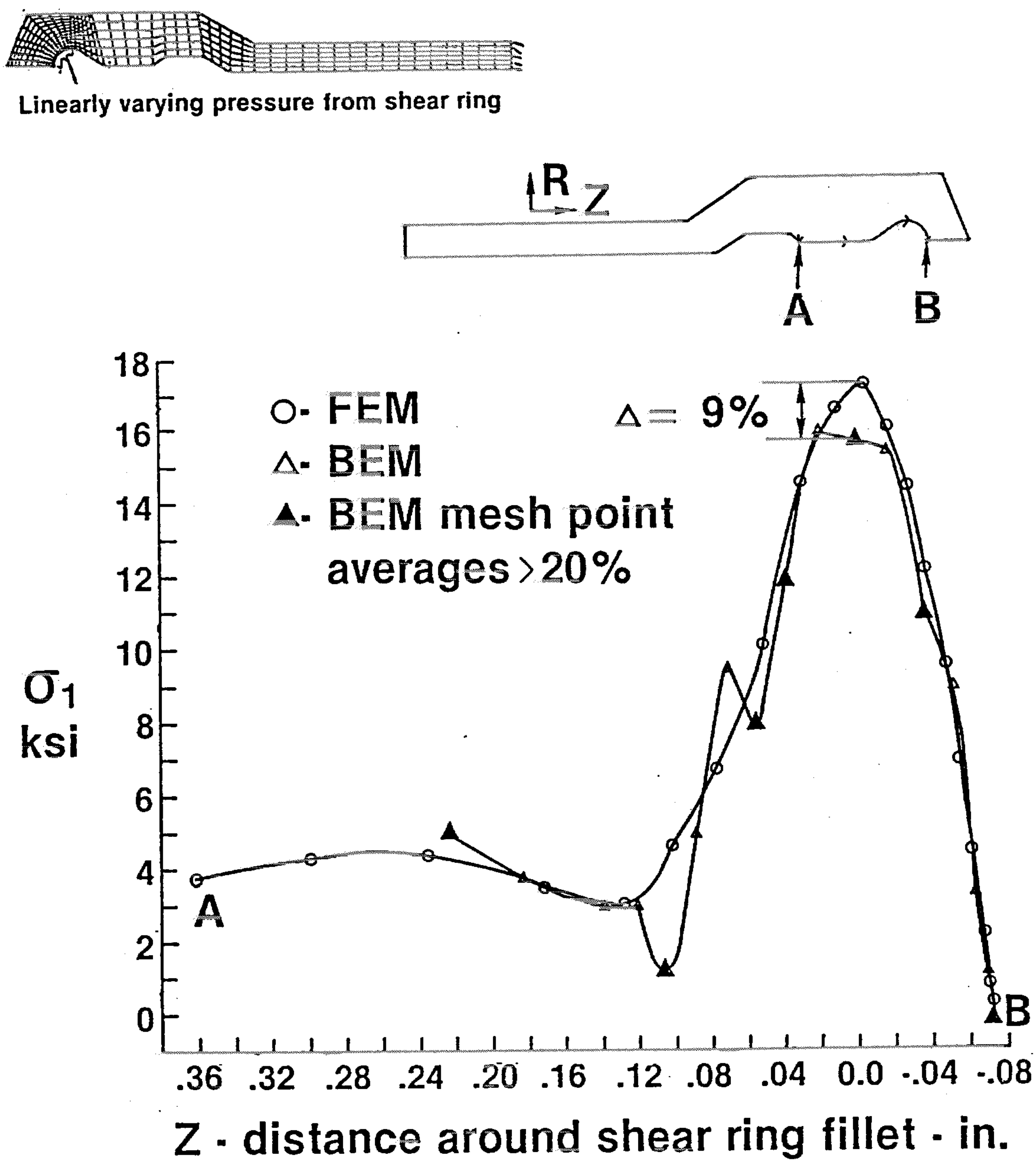

FIGURE 8

ACTUATOR COVER SURFACE STRESS

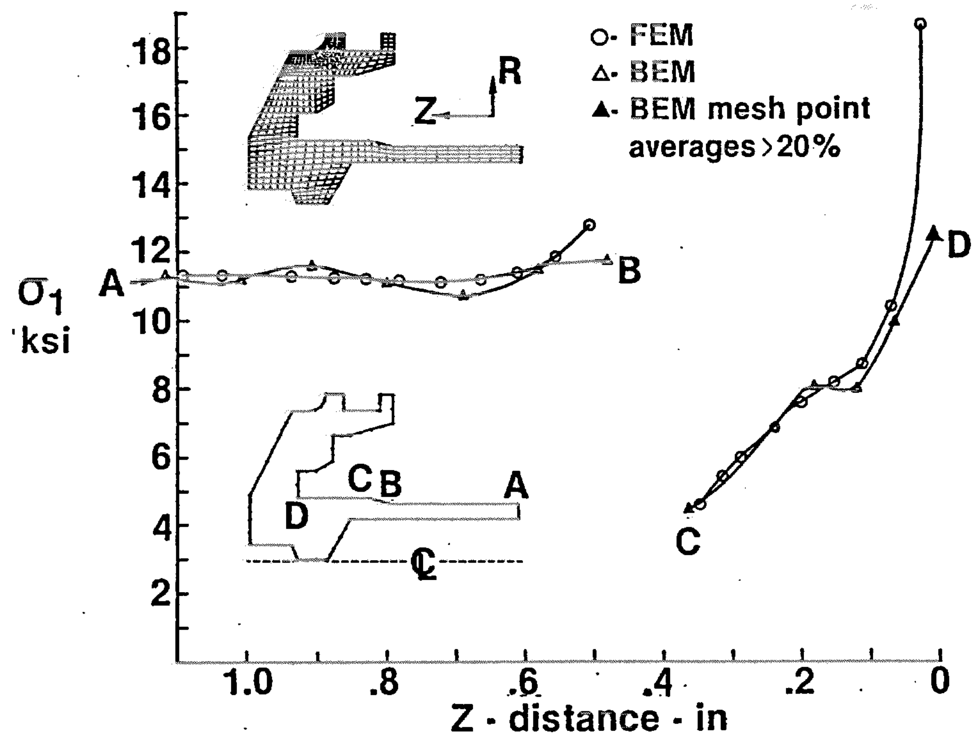

FIGURE 9

ACTUATOR COVER SURFACE STRESS

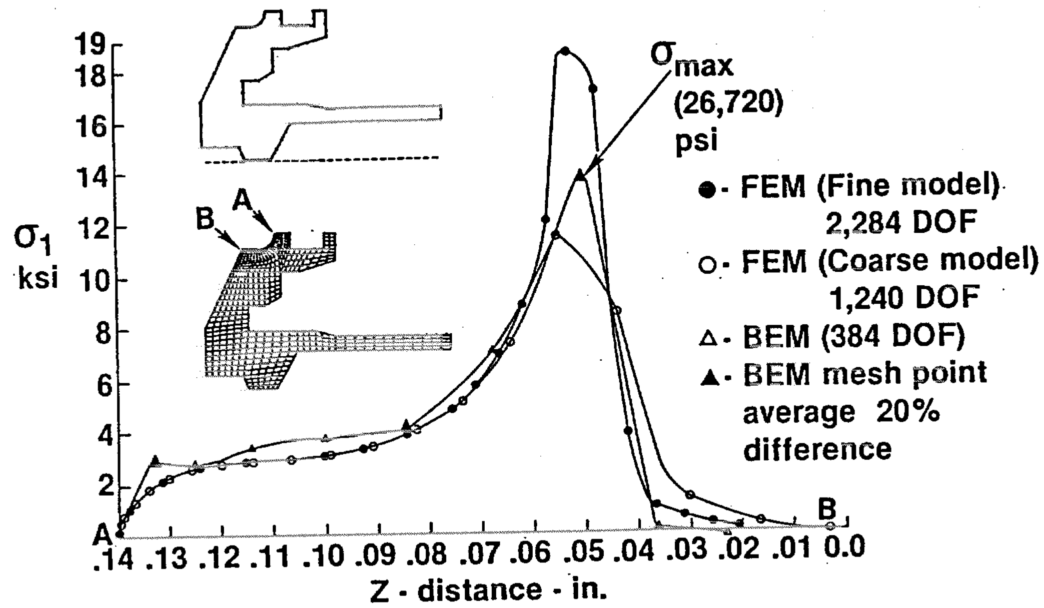

FIGURE 10

TOOTH FILLET SURFACE STRESS

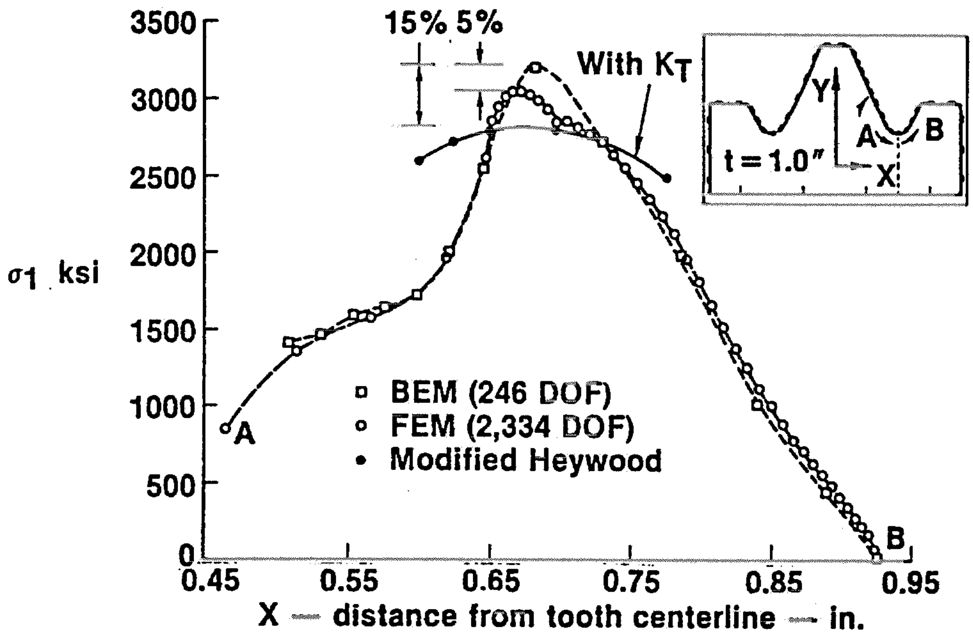

FIGURE 11

INTERNAL TOOTH STRESS

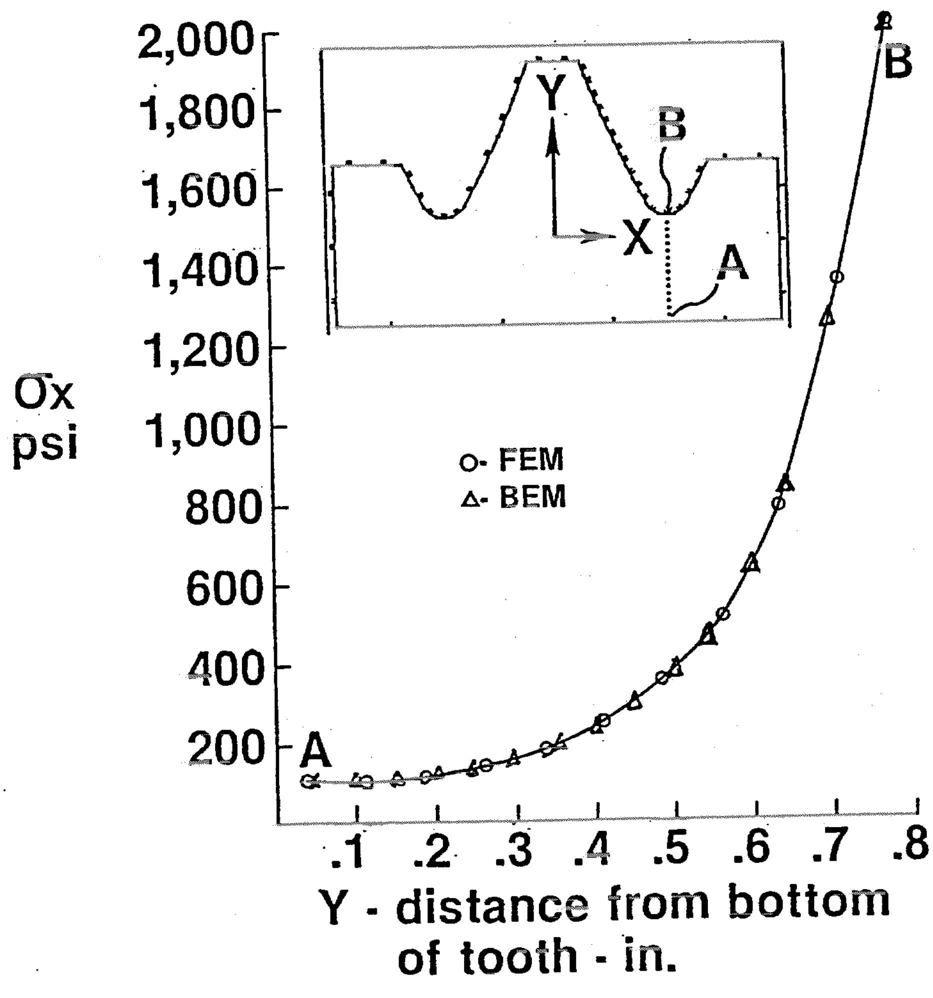

FIGURE 12

2D MODELING AND SOLUTION TIME

Analysis	Method	Model generation time (min.)	Lines of input	Solution time CPU (sec)
Internal spur gear tooth	FEM	60	130	18
	BEM	20	33	19
Actuator barrel	FEM	40	57	9
	BEM	10	36	12
Actuator cover	FEM	40	73	32
	BEM	15	61	93

FIGURE 13

FINITE ELEMENT TOOTH MODELS

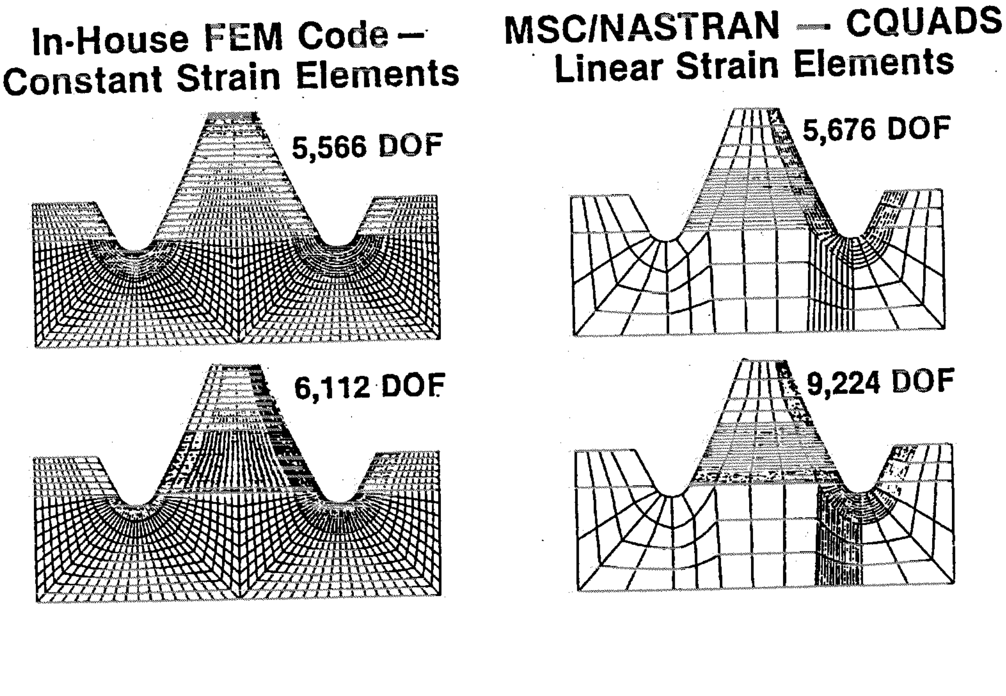

FIGURE 14

MAXIMUM STRESS CONVERGENCE FOR TOOTH MODEL

Code	Size (DOF)	CPU (sec)	σ max (psi)	Δ %
BEM-Beasy	246	19	3,210	-
	444	112	3,184	0.8
	528	164	3,193	0.3
FEM-in-house	2,334	18	3,053	-
	5,566	67	3,374	10.5
	6,112	61	3,232	4.2
FEM-MSC/ Nastran	5,676	164	3,260	-
	9,224	280	3,299	1.2

FIGURE 15

3D CYLINDER STRESS SUMMARY

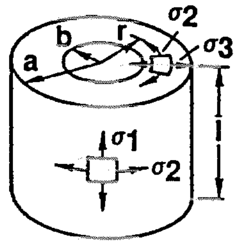

Computer Code	Analytical Method	Size DOF	Solution Time CPU (sec)	At r=b			
				σ_1 (psi)	σ_2 (psi)	σ_3 (psi)	Δb (in.)
—	Strength of materials (Roark)		—	0	133	−100	1.63E-7
BEASY	BEM	81 162 351	150 95 240	5 5 8	161 161 131	−147 −139 −105	1.86E-7 1.70E-7 1.69E-7
MSC/NASTRAN	FEM	579 2664 4500	20 184 331	14 5 3	141 136 134	−63 −88 −94	1.69E-7 1.65E-7 1.66E-7